Relaxation Time of High-Density Amorphous Ice

Philip H. Handle, Markus Seidl, and Thomas Loerting*

Institute of Physical Chemistry, University of Innsbruck, Innrain 52a, A-6020 Innsbruck, Austria

(Received 20 January 2012; published 31 May 2012)

Amorphous water plays a fundamental role in astrophysics, cryoelectron microscopy, hydration of matter, and our understanding of anomalous liquid water properties. Yet, the characteristics of the relaxation processes taking place in high-density amorphous ice (HDA) are unknown. We here reveal that the relaxation processes in HDA at 110–135 K at 0.1–0.2 GPa are of collective and global nature, resembling the alpha relaxation in glassy material. Measured relaxation times suggest liquid-like relaxation characteristics in the vicinity of the crystallization temperature at 145 K. By carefully relaxing pressurized HDA for several hours at 135 K, we produce a state that is closer to the ideal glass state than all HDA states discussed so far in literature.

DOI: 10.1103/PhysRevLett.108.225901 PACS numbers: 65.60.+a, 62.50.−p, 64.60.My, 64.70.P−

Water behaves as a simple liquid at high temperature and high pressure but becomes increasingly anomalous at low temperature and low pressure [1]. Dynamic properties of cold water show extrema at 0.1–0.2 GPa rather than simple linear behavior. Some attribute this to the appearance of an experimentally elusive high-density liquid at 0.2 GPa, which is structurally related to high-density amorphous ice (HDA) [2]. Yet, the question of whether HDA transforms to a supercooled liquid [3–6] or behaves like a crystal [7–10] upon heating at 0.1–0.2 GPa is disputed. Here, we analyze the relaxation of HDA by keeping it isothermally and isobarically at 0.1 or 0.2 GPa and 110–135 K and probing thermal stability at ambient pressure. Relaxation times obtained in this temperature interval suggest liquid-like relaxation times of <100 s at about 145 K. The HDA state presented here exhibits the highest thermal stability known so far.

Polyamorphism is used as a key concept in models aimed at understanding water's anomalous properties and as such forms the basis of the singularity-free scenario and the second-critical-point scenario [1]. The term ''polyamorphism'' arose after Mishima, Calvert, and Whalley discovered that crystalline ice I can be transformed to an amorphous form called high-density amorphous ice by applying pressure exceeding 1.1 GPa at 77 K [11]. HDA can subsequently be transformed to two additional amorphous forms, namely, low-density (LDA) [12] and very high-density amorphous ice (VHDA) [13]. These can be prepared by heating HDA to $T \geq 140$ K at low ($p < 0.1$ GPa) and high pressure ($p > 0.8$ GPa), respectively. Initiated by the seminal work of Nelmes *et al.,* our understanding of especially HDA has changed over the last few years [14]. It has been recognized since then that HDA prepared using the ''traditional'' recipe by Mishima, Calvert, and Whalley [11] represents a highly unrelaxed, strained form of HDA, denoted ''unannealed HDA'' (uHDA). By contrast, relaxed forms of HDA can be prepared by heating HDA at ambient [15] and elevated pressures [14,16] or by decompressing VHDA to intermediate pressure at 140 K [17]. Relaxed forms obtained at $p \leq 0.2$ GPa are denoted ''expanded HDA'' (eHDA) because the release of strain results in a slightly lower density of eHDA compared with that of uHDA.

At ambient pressure, cryoflotation indicates a density difference between uHDA and eHDA of 0.02 g cm^{-3} [18]. This density difference is evident in the volumetry curves depicted in Fig. 1(a). At 80 K the volume difference between uHDA and LDA is slightly larger than the volume difference between eHDA and LDA. Furthermore, uHDA expands much more with increasing temperature than eHDA does, reflecting its higher thermal expansivity. eHDA shows a thermal expansivity comparable to that of high-pressure ice polymorphs such as ice II, whereas uHDA expands much more than a crystalline polymorph [cf. slopes at 80–120 K in Fig. 1(a)]. This demonstrates its strained nature and the ability of uHDA to relax when the temperature is raised, whereas in eHDA more or less no reduction of stress is possible since it is well relaxed from the start. However, the topology, connectivity, and coordination number in the amorphous network of water molecules are similar in eHDA and uHDA, as indicated by powder neutron and x-ray diffraction studies [19]. The difference in the state of relaxation governs the thermal stability of HDA at ambient pressure, where eHDA can be heated to higher temperature than uHDA before transition to LDA takes place [14,20,21]. The higher thermal stability of eHDA is clearly seen in the volumetry curves [Fig. 1(a)] and in differential scanning calorimetry traces [Fig. 1(b)]. In volumetry conducted at 4 MPa and a heating rate of 3 K min^{-1}, eHDA is more resistive to transformation to LDA than uHDA by about 13 K [Fig. 1(a)], and in calorimetry conducted at ambient pressure (0.1 MPa) and a heating rate of 10 K min^{-1}, even by about 20 K [Fig. 1(b)]. Another noteworthy fact is that the location of the second exotherm in Fig. 1(b), corresponding to the crystallization of LDA to cubic ice, does not depend on the history of the

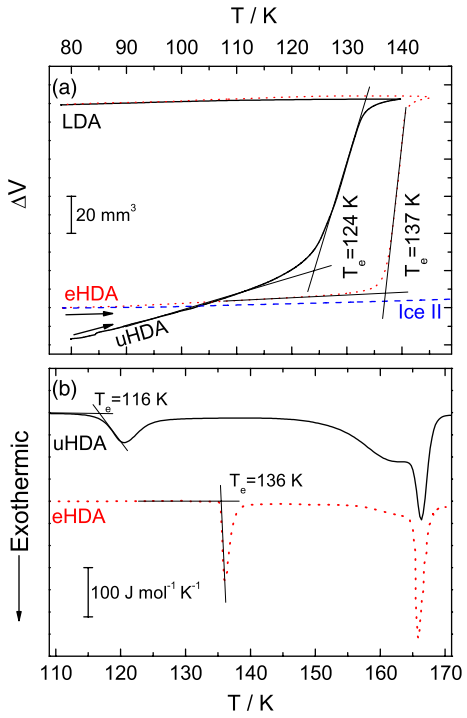

FIG. 1 (color online). Difference in the thermal stability of uHDA (produced along Mishima's path [11]) and eHDA (produced along Winkel's path [17]). Part (a) shows the volumetric detection of the isobaric ($p = 4$ MPa) transitions from 500 mg of uHDA (black solid line) and 500 mg of eHDA (red dotted line) to LDA, with a heating rate of 3 K min^{-1}. In this case, T_e represents the volumetric extrapolated onset transition temperature. The blue dashed line is the thermal expansion curve of ice II. Part (b) shows thermograms of uHDA (black solid line) and eHDA (red dotted line) recorded at 10 K min^{-1} heating rate. The first peak in the thermograms marks the exothermic HDA → LDA, and the second peak marks the exothermic LDA → I_c transition. Here, T_e represents the calorimetric extrapolated onset transition temperature.

sample in general and the annealing time in particular [see Fig. 1(b)]. This corroborates that the calorimetric onset temperature T_e of the first exotherm (HDA → LDA) is indeed a suitable probe of the relaxation state (for a detailed definition of the calorimetric T_e, cf. Refs. [21,22]).

While the differing degree of relaxation in uHDA and eHDA is qualitatively recognized, for example, by *in situ* Raman measurements provided by Yoshimura, Mao, and Hemley [23] and dielectric relaxation time measurements at elevated pressures by Andersson and Inaba [4,24], fundamental quantitative information is scarce. Most notably there is no quantitative information about structural relaxation times available, which is required in order to assess the merits of hypotheses such as the liquid–liquid transition scenario or the fragile-to-strong transition in supercooled water. Thus, we show here how the state of relaxation of uHDA develops with time while keeping a sample under isothermal and isobaric conditions in a piston cylinder setup for times of up to three hours (for apparatus details cf. Ref. [25]). The relaxation state is probed by means of the HDA → LDA transition temperature, observed in *ex situ* differential scanning calorimetry experiments, which is a novel approach developed in our group [21]. The suitability of *ex situ* characterization, the so-called quench recovery procedure, is documented elsewhere [26]. Using this approach we extract alpha relaxation times of HDA at 0.1 and 0.2 GPa. The relaxation process as investigated by the analysis of thermal stability is a long-range, global process rather than the short-range relaxation process studied previously by Raman spectroscopy [16,23]. Therefore, for the first time a dynamic property of HDA, which is directly linked to the viscosity, is measured below the glass transition temperature, i.e., beyond the usual scope of the Angell plot ($\frac{T_g}{T} > 1$) [27].

The large difference in thermal stability at ambient pressure between uHDA and eHDA makes calorimetry a highly sensitive tool suitable for the study of the state of relaxation of HDA, whereas diffraction methods are much less sensitive, because the static structure factor barely changes upon relaxation of HDA. Progressively relaxed HDA samples have been obtained by heating uHDA at 0.1 or 0.2 GPa to 110, 125, 130, or 135 K and by keeping them under isobaric and isothermal conditions for times in the range from 1 s to approximately 3 h. Attempts to study the relaxation behavior with higher temperature as well, e.g., 140 K, have been unsuccessful because of complete crystallization of HDA kept under these conditions [28–30]. Figure 2 exemplarily shows the progressive shift to a more relaxed state with time

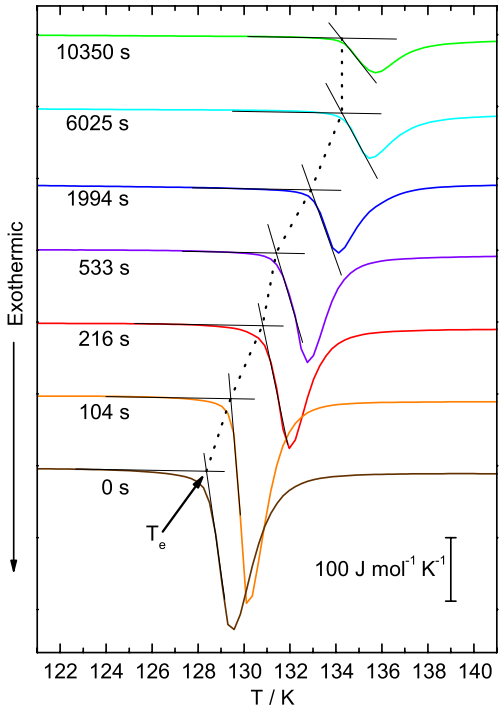

FIG. 2 (color online). *Ex situ* characterization of the state of relaxation of HDA samples after having kept them at 0.1 GPa and 130 K for the indicated times. Note that T_e shifts progressively to higher temperature (dotted black line).

by keeping the sample for up to approximately 3 h at 0.1 GPa and 130 K. In general, the HDA → LDA onset temperature T_e (cf. arrow in Fig. 2) as a function of annealing time shows an exponential shape and asymptotically approaches a value of 136 K, which is the highest onset temperature ever measured for the transformation of HDA to LDA at ambient pressure. We, therefore, regard a sample showing a T_e of 136 K to be entirely relaxed.

Figure 3 summarizes all onset temperatures T_e extracted from the calorimetry data as a function of time in a manner analogous to the one shown in Fig. 2. It is immediately evident that longer annealing times result in higher onset temperatures and, thus, in a higher degree of relaxation. It is also immediately evident that same annealing times result in more relaxed samples when annealed at higher temperature. To extract the relaxation time from the data we use the function

$$T_e(t) = T_{e,\infty} + (T_{e,0} - T_{e,\infty})e^{-(t/\tau)^n}, \quad (1)$$

where T_e is the HDA → LDA transition temperature, and n and τ (the relaxation time) are fitting parameters. $T_{e,0}$ is the lowest transition temperature of the respective data set, and $T_{e,\infty}$ is 136 K, since samples showing $T_e = 136$ K are considered fully relaxed, whereas the state obtained after 0 s annealing time is considered unrelaxed. The relaxation times extracted from the data sets at 110–135 K are depicted in Fig. 4 as an Arrhenius-type plot. The standard relative error in relaxation times is about 10–50% at 125–135 K and larger at 110 K because the relaxation times at 110 K are $>10^6$ s, which is far beyond the time scale of the experiment. Using a relaxation time of 100 s to define the glass transition temperature T_g, an Arrhenius-type fit to the data yields an extrapolated $T_g(0.1\ \text{GPa}) = 144 \pm 2$ K and $T_g(0.2\ \text{GPa}) = 150 \pm 11.5$ K [cf. red dashed lines in Figs. 4(a) and 4(b) and stars in Fig. 4(c)]. The standard error of T_g reflects the uncertainty of the linear regression (67%), which takes into account the error bars on the relaxation times. In addition, we also analyzed our results by fitting T_e vs ln$t$ data linearly, in analogy to the approach used by Koza *et al.* [31]. We have found that a line fits the data quite well, and the T_g's extracted using this approach are identical within the error bars. The T_g extracted by extrapolation from the *ex situ* measurements of relaxation times here agrees well with the T_g extracted by using an *in situ* dilatometric approach [6] [Fig. 4(c), filled

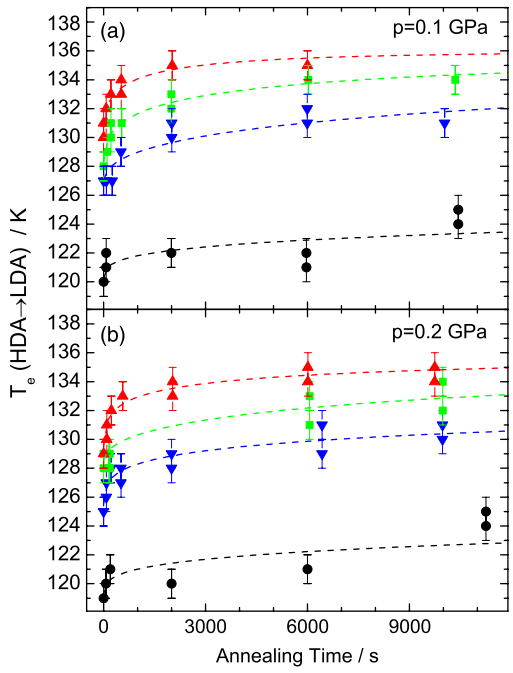

FIG. 3 (color online). Collection of all calorimetric HDA → LDA transition temperatures T_e for (a) 0.1 GPa and (b) 0.2 GPa. In each panel, the temperatures T_e are represented as (•) for samples annealed at 110 K, (▼) for samples annealed at 125 K, (■) for samples annealed at 130 K, and (▲) for samples annealed at 135 K. The dashed curves are the fits according to Eq. (1). In both (a) and (b) all transition values of T_e have an error of ±1 K.

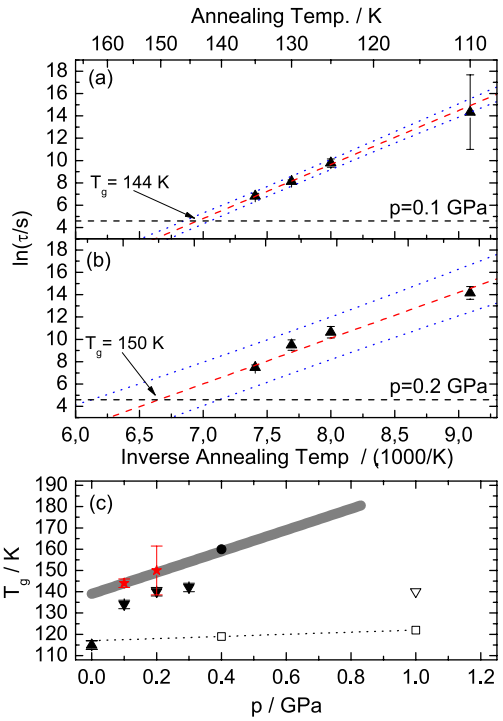

FIG. 4 (color online). Parts (a) and (b) show Arrhenius plots of relaxation times τ of uHDA (represented by ▲), as calculated from Eq. (1) and the data shown in Fig. 3. Relaxation times for 0.1 GPa in part (a) and for 0.2 GPa in part (b). The red dashed line is the Arrhenius fit, the blue dotted lines are the prediction bands (67%), and the black dashed line ($\tau = 100$ s) marks the transition from a glass (above the line) to a liquid (beneath the line). Part (c) shows the glass transition temperatures T_g obtained in this study (★) in comparison with data from literature: Seidl *et al.* [6], calorimetry (▲); Seidl *et al.* [6], volumetry (▼); Andersson, transient hot-wire method [5] (▽); Mishima, temperature change in emulsified water [3] (•) and gray area (Mishima's extrapolation); Andersson and Inaba, dielectric spectroscopy [4] (□) and dotted line (Andersson's extrapolation).

downward triangles]. It also coincides with the values obtained by Mishima with emulsified water [3] [Fig. 4(c), circle and gray bar]. T_g's reported by Andersson and Inaba using dielectric relaxation spectroscopy [4,24] [Fig. 4(c), open squares], high-pressure calorimetry, and thermal conductivity measurements [Fig. 4(c), open triangle] [5] are somewhat lower than the data by Mishima [3] and our own data. We attribute this to the fact that Andersson probably studied VHDA rather than HDA. The data in Figs. 4(a) and 4(b) imply activation energies for the relaxation process of 40 kJ mol^{-1} at 0.1 GPa and 34 kJ mol^{-1} at 0.2 GPa, which is in reasonable agreement with the value of 45 kJ mol^{-1} at 1.0 GPa obtained by Andersson and Inaba for a VHDA sample [4].

In conclusion, we have shown that the state of relaxation in HDA is a very important property, which has not received sufficient attention in the previous literature. By probing the state of relaxation using differential scanning calorimetry we are able to follow the relaxation process from the highly strained uHDA state to the well relaxed eHDA state. Our results show that the relaxation time drops rapidly from $>10^6$ s at 110 K to approximately 10^3 s at 135 K, which implies T_g values for HDA of 144 and 150 K at 0.1 and 0.2 GPa, respectively. Furthermore, this emphasises the role of eHDA (produced along Winkel's path [17]) as a proxy of a high-density liquid in the context of a possible two- or multi-liquid nature of water. The long-range relaxation process occurring when uHDA transforms to eHDA affects properties such as the phonon density of states. We speculate that the crystal-like phonons observed in uHDA [9,10] and similarities to high-pressure ice phases such as ice VI [7] might no longer be observable in eHDA by inelastic neutron-scattering experiments. Finally, whereas uHDA has been regarded as a mixture of highly strained high-pressure phases of ice [8], eHDA can not be regarded as such a mixture because of its relaxed nature. Our experiments rather suggest that the eHDA, which transforms at 136 K to LDA, can be be regarded as being close to an ideal glassy state in the sense that its excess entropy and excess enthalpy are very low because of the hours of annealing slightly below T_g [27].

P. H. H. thanks W. Stadlmayr for fruitful discussions. The authors also thank M. Bauer, K. Handle, N. Memmel, F. Neumann, R. Pramsoller, and W. Stadlmayr for technical support during the relocation of our DSC apparatus. Furthermore, we are grateful to the European Research Council (ERC Starting Grant SULIWA to T. L.) and the Austrian Academy of Sciences (M. S.) for financial support.

*thomas.loerting@uibk.ac.at

[1] P. G. Debenedetti, J. Phys. Condens. Matter **15**, R1669 (2003).
[2] O. Mishima and H. E. Stanley, Nature (London) **396**, 329 (1998).
[3] O. Mishima, J. Chem. Phys. **121**, 3161 (2004).
[4] O. Andersson and A. Inaba, Phys. Rev. B **74**, 184201 (2006).
[5] O. Andersson, Proc. Natl. Acad. Sci. U.S.A. **108**, 11 013 (2011).
[6] M. Seidl, M. S. Elsaesser, K. Winkel, G. Zifferer, E. Mayer, and T. Loerting, Phys. Rev. B **83**, 100201 (2011).
[7] A. I. Kolesnikov, V. V. Sinitsyn, E. G. Ponyatovsky, I. Natkaniec, and L. S. Smirnov, Physica (Amsterdam) **213B–214B**, 474 (1995).
[8] G. P. Johari, Phys. Chem. Chem. Phys. **2**, 1567 (2000).
[9] H. Schober, M. M. Koza, A. Tölle, C. Masciovecchio, F. Sette, and F. Fujara, Phys. Rev. Lett. **85**, 4100 (2000).
[10] R. V. Belosludov, O. S. Subbotin, H. Mizuseki, P. M. Rodger, Y. Kawazoe, and V. R. Belosludov, J. Chem. Phys. **129**, 114507 (2008).
[11] O. Mishima, L. D. Calvert, and E. Whalley, Nature (London) **310**, 393 (1984).
[12] O. Mishima, L. D. Calvert, and E. Whalley, Nature (London) **314**, 76 (1985).
[13] T. Loerting, C. Salzmann, I. Kohl, E. Mayer, and A. Hallbrucker, Phys. Chem. Chem. Phys. **3**, 5355 (2001).
[14] R. J. Nelmes, J. S. Loveday, T. Straessle, C. L. Bull, M. Guthrie, G. Hamel, and S. Klotz, Nature Phys. **2**, 414 (2006).
[15] C. A. Tulk, C. J. Benmore, J. Urquidi, D. D. Klug, J. Neuefeind, B. Tomberli, and P. A. Egelstaff, Science **297**, 1320 (2002).
[16] C. G. Salzmann, T. Loerting, S. Klotz, P. W. Mirwald, A. Hallbrucker, and E. Mayer, Phys. Chem. Chem. Phys. **8**, 386 (2006).
[17] K. Winkel, M. S. Elsaesser, E. Mayer, and T. Loerting, J. Chem. Phys. **128**, 044510 (2008).
[18] T. Loerting, M. Bauer, I. Kohl, K. Watschinger, K. Winkel, and E. Mayer, J. Phys. Chem. B **115**, 14 167 (2011).
[19] T. Loerting, K. Winkel, M. Seidl, M. Bauer, C. Mitterdorfer, P. H. Handle, C. G. Salzmann, E. Mayer, J. L. Finney, and D. T. Bowron, Phys. Chem. Chem. Phys. **13**, 8783 (2011).
[20] O. Mishima, Nature (London) **384**, 546 (1996).
[21] K. Winkel, E. Mayer, and T. Loerting, J. Phys. Chem. B **115**, 14 141 (2011).
[22] G. W. H. Höhne, W. Hemminger, and H.-J. Flammersheim, *Differential Scanning Calorimetry: An Introduction for Practitioners* (Springer-Verlag, Berlin, 1996).
[23] Y. Yoshimura, H. kwang Mao, and R. J. Hemley, J. Raman Spectrosc. **41**, 678 (2009).
[24] O. Andersson, Phys. Rev. Lett. **95**, 205503 (2005).
[25] M. S. Elsaesser, I. Kohl, E. Mayer, and T. Loerting, J. Phys. Chem. B **111**, 8038 (2007).
[26] M. Bauer, K. Winkel, D. M. Toebbens, E. Mayer, and T. Loerting, J. Chem. Phys. **131**, 224514 (2009).
[27] C. A. Angell and W. Sichina, Ann. N.Y. Acad. Sci. **279**, 53 (1976).
[28] O. Mishima, J. Chem. Phys. **100**, 5910 (1994).
[29] E. L. Gromnitskaya, O. V. Stal'gorova, V. V. Brazhkin, and A. G. Lyapin, Phys. Rev. B **64**, 094205 (2001).
[30] M. Seidl, K. Winkel, P. H. Handle, G. Zifferer, E. Mayer, and T. Loerting, in *Proceedings of the Eighth Liquid Matter Conference—Conference Book* (European Physical Society, Groningen, The Netherlands, 2011).
[31] M. M. Koza, H. Schober, H. E. Fischer, T. Hansen, and F. Fujara, J. Phys. Condens. Matter **15**, 321 (2003).